Green Chemistry

Accepted Manuscript

This is an *Accepted Manuscript*, which has been through the Royal Society of Chemistry peer review process and has been accepted for publication.

Accepted Manuscripts are published online shortly after acceptance, before technical editing, formatting and proof reading. Using this free service, authors can make their results available to the community, in citable form, before we publish the edited article. We will replace this *Accepted Manuscript* with the edited and formatted *Advance Article* as soon as it is available.

You can find more information about *Accepted Manuscripts* in the Information for Authors.

Please note that technical editing may introduce minor changes to the text and/or graphics, which may alter content. The journal's standard Terms & Conditions and the Ethical guidelines still apply. In no event shall the Royal Society of Chemistry be held responsible for any errors or omissions in this *Accepted Manuscript* or any consequences arising from the use of any information it contains.

ROYAL SOCIETY OF CHEMISTRY

www.rsc.org/greenchem

Synergetic Catalysis of Palladium Nanoparticles Encaged within Amine-functionalized UiO-66 in Hydrodeoxygenation of Vanillin in Water

Fumin Zhang,*[ab] Shuang Zheng,[a] Qiang Xiao,[a] Yijun Zhong,[a] Weidong Zhu,[a] Andrew Lin,[b] and M. Samy El-Shall*[b]

[a]Key Laboratory of the Ministry of Education for Advanced Catalysis Materials, Institute of Physical Chemistry, Zhejiang Normal University, 321004 Jinhua, People's Republic of China
[b]Department of Chemistry, Virginia Commonwealth University, 23284 Richmond, VA, United States

Corresponding Authors: Tel.: +86 579 82288919; Fax: +86 579 82282234; E-mail: zhangfumin@zjnu.edu.cn, fzhang5@vcu.edu (F. Zhang), mselshal@vcu.edu (M. Samy El-Shall).

ABSTRACT

Ultrasmall palladium nanoparticles (1.5 - 2.5 nm) encapsulated in metal−organic frameworks (MOFs) have been prepared by introducing a palladium precursor into a highly porous and hydrothermally stable amine-functionalized UiO-66 (NH_2-UiO-66) via direct anionic exchange and subsequent H_2 reduction. The prepared Pd@NH_2-UiO-66 catalyst was then applied in the hydrodeoxygenation of vanillin (a typical model compound of lignin) at low H_2 pressure in aqueous media. Excellent catalytic results (100% conversion of vanillin with exclusive selectivity for 2-methoxy-4-methylphenol) could be achieved over the developed 2.0 wt.% Pd@NH_2-UiO-66 catalyst under mild conditions. Furthermore, the catalytic activity and selectivity were not affected after six reaction cycles indicating excellent stability and reproducibility of this catalyst system. It was found that the presence of free amine groups in the frameworks of NH_2-UiO-66 plays a key role in the formation of uniform, well-dispersed and leaching resistant palladium nanoparticles within the MOF host. Moreover, the developed Pd@NH_2-UiO-66 exhibits a novel synergetic catalysis in the hydrodeoxygenation due to the cooperation between the well-dispersed metallic Pd sites and the amine-functionalized MOF support, in which Pd offers hydrogenation activity and the MOF support facilitates hydrogenolysis of the intermediate vanillin alcohol to the 2-methoxy-4-methylphenol product.

KEYWORDS: Metal–organic frameworks; NH_2-UiO-66; Synergetic catalysis; Hydrodeoxygenation; Vanillin

Green Chemistry Accepted Manuscript

1. Introduction

The search for renewable and sustainable fuel sources has drawn great attention because of the continued depletion of fossil fuels [1]. The conversion of biomass into fuels and chemical feedstocks is an alternative to fossil fuels because of the availability and low cost of biomass [2]. Lignin, which constitutes ~30 wt.% of woody biomass, is one of the most abundant bio-sources on earth [3]. Compared to cellulose-derived pyrolysis oil, it is more challenging to deoxygenate lignin-derived pyrolysis oil due to its highly complex structure, which consists of oxygen-rich subunits derived from phenol, *p*-coumaryl, coniferyl, and sinapyl alcohols typically connected with ether linkages [4]. Catalytic hydrodeoxygenation is considered to be the most important and feasible strategy to upgrade the quality of biofuels [5-8]. Various heterogeneous catalysts, mainly those consisting of supported noble metal catalysts such as Pt-Ni/γ-Al_2O_3 [9], Pt-Co/γ-Al_2O_3[9], Pd/γ-Al_2O_3 [10], Pd/TiO_2 [10], Pd/MgO [10], Pd/CeO_2 [10], Pd/C [10], Pd/N-doped carbon [10], Ru/CNT [11], Au/CNTs [12], Pd/carbonaceous microspheres [13], Pd/SWNT-SiO_2 [14], and Pd/MSMF (MSMF: superhydrophilic mesoporous sulfonated melamine–formaldehyde resin) [15], have been tested in the hydrodeoxygenation of biomass compounds. In addiction, hydrodeoxygenation of anisole, a methoxy-rich lignin model compound, has been investigated over a series of Ni-containing catalysts supported on activated carbon, SBA-15, SiO_2, and γ-Al_2O_3 [16], and the cleavage of lignin-derived 4-O-5 aryl ethers has also been conducted over Ni nanoparticles supported on niobic acid-activated carbon composite [17]. However, many of these catalysts exhibited low catalytic activity and poor reusability. Therefore, the development of highly active and stable catalysts for the hydrodeoxygenation is desirably required.

Metal–organic frameworks (MOFs) represent a new class of porous materials assembled from inorganic nodes and organic linkers [18,19]. Due to their well-ordered crystalline structure, high porosity, tunable pore size, and modifiable surface properties, the applications of MOFs in heterogeneous catalysis have recently attracted tremendous attention [20,21], particularly, those using MOFs as supports for noble metal (e.g., Pd, Au, Ru, and Pt) nanoparticles [22-36]. Despite the many investigations of the MOFs' role in catalysis, there are only a limited number of studies of bifunctional metal@MOFs systems for tandem catalysis [37-43]. For example, Pan *et al.* prepared Pd@MIL-101 for the one-pot synthesis of methyl isobutyl ketone from acetone [37]; Zhao *et al*.

Green Chemistry Accepted Manuscript

designed a core−shell Pd@IRMOF-3 and used it as a multifunctional catalyst for a cascade condensation-hydrogenation reaction [40]; recently, Chen *et al.* developed a multifunctional PdAg@MIL-101 for one-pot multistep cascade conversion of nitroarene to secondary arylamine through the combination of host-guest cooperation and guest bimetallic synergy [41]. In light of these reports, the development of MOFs-based multifunctional materials for tandem catalysis will exert a significant impact on conventional chemical industrial processes [44,45].

The metal-organic framework UiO-66 is built up from $[Zr_6O_4(OH)_4(CO_2)_{12}]$ clusters linked with 1,4-benzenedicarboxylic acid [46,47]. The framework is comprised of tetrahedral and octahedral cages, in a 2:1 ratio, with diameters close to 0.75 and 1.2 nm, respectively. Access to these cages is provided by narrow triangular windows with a diameter close to 0.6 nm [46,47]. UiO-66 and its amin-functionalized isostructure NH_2-UiO-66 show great potential for many applications due to their good thermal stability, resistance toward a variety of organic solvents as well as acidic and basic aqueous media [48-51]. Besides the above mentioned features, NH_2-UiO-66, as a host matrix to support nanoparticle catalysts, has several unique characteristics including [27,28,43,46]: i) the large pore volume of NH_2-UiO-66 is appropriate for the loading of metal precursors, ii) the amine groups on terephthalic acid linkers in NH_2-UiO-66 could provide coordination sites for metal ions, and iii) NH_2-UiO-66 possesses numerous potentially unsaturated metal Zr sites having Lewis acidity upon activation in vacuum. The Lewis acidity of the NH_2-UiO-66 support has been demonstrated to play significant roles in promoting the reactivity of aromatic substrates [48-51].

In this paper, we report the development of a new catalyst system consisting of Pd nanoparticles incorporated within the NH_2-UiO-66 framework by using a direct anionic exchange and subsequent gentle reduction approach. The developed 2.0 wt.% Pd@NH_2-UiO-66 catalyst shows excellent catalytic properties in the hydrodeoxygenation of vanillin (a typical model compound of lignin), as a model reaction to explore the principal hydrogenation and hydrogenolysis routes (Scheme 1), due to the synergistic catalysis between the MOF host and the metal nanoparticles guest. The MOF promotes transformation of the intermediate vanillin alcohol formed in situ, while Pd nanoparticles offer hydrogenation activity, much superior to the analogue catalysts reported in the literature.

Green Chemistry Accepted Manuscript

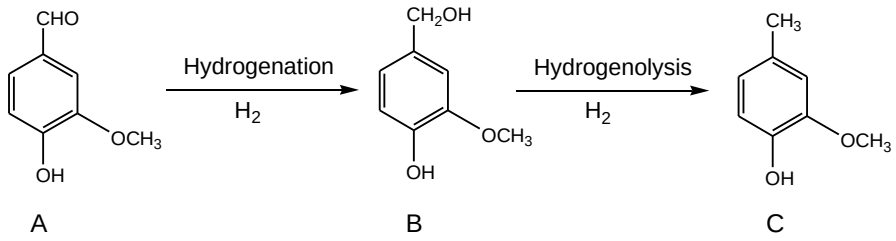

Scheme 1. Possible reaction pathways for hydrodeoxygenation of vanillin (A) to 2-methoxy-4-methylphenol (C).

2. Experimental section

2.1. Chemicals

All reagents with AR purity (analytical reagent grade) were purchased and used as received without further purification. Deionized water with a resistance larger than 18.2 MΩ was obtained from a Millipore Milli-Q ultrapure water purification system.

2.2. Catalyst preparation

The synthesis of NH_2-UiO-66 was based on the procedure reported by Lillerud and coworkers with some modification [46]. Typcially, $ZrCl_4$ (0.24 g, 1.029 mmol) was dissolved in 60 mL of N,N′-dimethylformamide (DMF) by sonication for 5 min. Then, the ligand 2-aminoterephthalic acid (0.186 g, 1.029 mmol) and 0.15 mL deionized water were added into the clear solution under vigorous stirring for 10 min at room temperature. Aftwards, the solution was transferred into a teflon-lined stainless steel autoclave. The tightly capped autoclave was kept in an oven at 120 °C under static conditions. After 24 h, the solutions were cooled to room temperature and the precipitates were isolated by centrifugation. The solids were washed with 40 mL of DMF three times and followed by washing with 40 mL of methanol three times. During each wash, the suspension was kept at room temperature for 24 h before being centrifuged. The solvent was decanted. Finally, the solids were dried at 150 °C under vacuum. Pure UiO-66, was synthesized by the same method as aforementioned for the preparation of NH_2-UiO-66 by using terephthalic acid as the organic ligand.

To prepare 2.0 wt.% Pd@NH_2-UiO-66, 0.5 g of vacuum-dried NH_2-UiO-66 was first dispersed in 30 mL of deionized water at room temperature, and treated with appropriate amount of hydrochloric acid to tune the pH of the slurry around 4. Then 1.68 mL aqueous H_2PdCl_4 (0.0552

Green Chemistry Accepted Manuscript

mol/L) was added dropwise to the above solution under vigorous stirring. The slurry was stirred at room temperature for 20 h. Then the impregnated NH_2-UiO-66 was washed with 30 mL of water three times by centrifugation and then dried at 80 °C in a vacuum desiccator for 10 h. The resulting dried sample, the Pd^{2+} impregnated NH_2-UiO-66 ($[NH_3^+$-UiO-66$]_2[PdCl_4]^{2-}$), was reduced in a 20% H_2/N_2 flow (H_2/N_2 = 10/40 mL/min) at 200 °C for 4 h to obtain Pd nanoparticles confined inside the cavities of NH_2-UiO-66. For controlled experiments and comparisons of catalyst's locations, Pd nanoparticles inside UiO-66, and Pd nanoparticles supported on the outer surface of UiO-66-NH_2 (the support UiO-66-NH_2 without purification by DMF and methanol) were also prepared by the same method.

2.3. Catalyst characterization

The X-ray powder diffraction (XRD) patterns were obtained on a Philips PW3040/60 diffractometer, using Cu$K\alpha$ radiation (λ = 0.1541 nm) in a scanning range of 5~50° at a scanning rate of 1°/min.

N_2 adsorption isotherms were obtained at -196 °C using a Micromeritics ASAP 2020 instrument. The samples were outgassed under vacuum at 150 °C for 10 h, prior to the adsorption measurements.

The amount of the Pd in NH_2-UiO-66 was measured by an IRIS Intrepid II XSP inductively coupled plasma-atomic emission spectrometer (ICP-AES). Because the emission of zirconium in NH_2-UiO-66 is similar to that of the palladium, it is difficult to detect the palladium amount directly by ICP-AES. Instead, we measured the amount of Pd that was washed away during the washing steps and calculated the actual palladium remaining in Pd@NH_2-UiO-66. When loading the 2.0 wt.% Pd in NH_2-UiO-66, the exact initial weight of the palladium precursor was recorded first. Every time after washing, the washing solution that contained the palladium residue was collected. Finally, ICP-AES was performed for the washing solution, and the palladium content was calculated. The difference between added and removed Pd (during washing steps) is the actual palladium amount that was introduced in NH_2-UiO-66. The same method was also used to determine the actual Pd amount in Pd@UiO-66.

The infrared (IR) spectra were collected on a Nicolet NEXUS670 Fourier transform IR

Green Chemistry Accepted Manuscript

spectrophotometer in KBr disks at room temperature.

The surface electronic states were investigated by X-ray photoelectron spectroscopy (XPS, Thermo VG ESCALAB250 using Al*Kα* radiation). The XPS data were internally calibrated, fixing the binding energy of C 1s at 284.6 eV.

Scanning electron microscopy (SEM) was performed on a Hitachi S-4800 apparatus which was performed on a sample powder previously dried and sputter-coated with a thin layer of gold. In addition, energy-dispersive X-ray spectroscopy (EDX) analyses were also performed to confirm the presence and the distribution of Pd nanoparticles.

The transmission electron microscopy (TEM) observations were carried out on a JEOL JEM-1200 working at 200 kV. The sample was diluted in ethanol to give a 1 : 5 volume ratio and sonicated for 10 min. The ethanol slurry was then dropped onto a Cu grid covered with a thin film of carbon.

Temperature-programmed desorption (TPD) profiles of NH_3 from the MOF catalysts were measured using a Micromeritics AutoChem II 2920 instrument. The sample cell loaded with 0.1 g of sample was initially treated in a helium flow of 40 mL/min at 200 °C for 2 h, then cooled to 100 °C, and subsequently exposed to pulses of ammonia until saturation and then purged with helium flow at 100 °C for 1 h. Afterwards, the sample cell was heated to 400 °C with a ramp of 10 °C/min. The concentration of the desorbed ammonia was monitored continuously with a TCD detector. The total amount of the desorbed NH_3 for the 2.0 wt.% Pd@NH_2-UiO-66 catalyst was determined by a reaction with an excess of dilute HCl solution and back titration with NaOH solution, according to the procedure described in our previous work [54].

2.4. Hydrodeoxygenation of vanillin

The catalytic hydrodeoxygenation of vanillin was carried out in a 50 ml Teflon-lined autoclave equipped with stirrer, heater, and sample port. In a typical experiment, 2 mmol of vanillin, 0.05 g of catalyst, and 20 ml water as solvent were charged into the autoclave and were repeatedly purged with hydrogen gas at room temperature. Afterwards, the autoclave was heated at 90 ºC and then pressurized with hydrogen up to 0.5 MPa. Finally, the agitation was initiated with a stirring speed of 1000 rpm. A steady pressure was maintained throughout the reaction period. The mixture was

Green Chemistry Accepted Manuscript

extracted with ethyl acetate and the catalyst was taken out from the system by centrifugation before being analyzed by GC (Agilent 6820) equipped with an FID detector and a capillary column (DB-5, 30 m × 0.45 mm × 0.42 μm). Additionally, the reaction conditions with respect to temperature, time, hydrogen pressure, and molar ratio of the catalyst amount to vanillin were studied.

In order to test the catalytic reusability of 2.0 wt.% Pd@NH_2-UiO-66, after the reaction, the catalyst was separated by filtration, washed with ethanol, and dried in a vacuum desiccator at 150 °C for 5 h, and then the recovered catalyst was used in the next run reaction.

2.5. Hydrogenation of *n*-hexylene and cyclooctene

The encapsulation of Pd nanoparticles in NH_2-UiO-66 was indirectly verified by the hydrogenation of *n*-hexylene and cyclooctene. Typically, 0.03 g catalyst, 2.0 mmol substrate, and 20 mL ethanol were added into a stainless steel autoclave. After replacing the air in the autoclave with argon, 2 MPa H_2 was injected, and the catalytic tests were then performed at 80 ^oC for 120 min. The products were analyzed by GC (Agilent 6820) with a OV-101 capillary column.

2.6. Adsorption Experiments

NH_2-UiO-66 and UiO-66 were dried at 150 °C under vacuum for 24 h before adsorption experiments. Adsorption of vanillin was investigated by addition of activated MOFs (0.05 g) to the solutions of vanillin (1.0 mmol) in water (100 ml). The mixture was stirred at 25 °C for 48 h. The amount of adsorbed vanillin over MOFs was determined by measuring the UV-vis spectra of the solution. The adsorption of vanillin alcohol over NH_2-UiO-66 and UiO-66 was performed with the same procedure to that of vanillin except that vanillin was replaced by vanillin alcohol.

3. Results and discussion

3.1. Catalyst characterization

Pd@NH_2-UiO-66 was prepared by incorporating a Pd precursor into the amine-functionalized metal-organic framework NH_2-UiO-66 via direct anionic exchange and subsequent H_2 reduction. The prepared catalysts were characterized by means of various techniques. As shown in the XRD patterns in Fig. 1, the encapsulation of Pd into NH_2-UiO-66 does not influence the crystallinity of the parent

Green Chemistry Accepted Manuscript

NH_2-UiO-66 and characteristic XRD peaks of Pd nanoparticles are not observed, mainly due to the low loading and high dispersion of the ultrasmall Pd nanoparticles inside the MOF matrix. Fig. 2 shows the N_2 adsorption isotherms of various catalysts at -196 °C, from which the textural properties were determined, and the results are summarized in Table S1. The specific surface area of Pd@NH_2-UiO-66 is 769.2 m^2/g with a micorpore volume of 0.35 cm^3/g, which are lower than those of unloaded NH_2-UiO-66 support (931.5 m^2/g with a micorpore volume of 0.38 cm^3/g). The decrease in the surface area and pore volume of Pd@NH_2-UiO-66, in comparison with those of NH_2-UiO-66, may be ascribed to the partial occupation of the cavities in NH_2-UiO-66 by the deposited Pd nanoparticles.

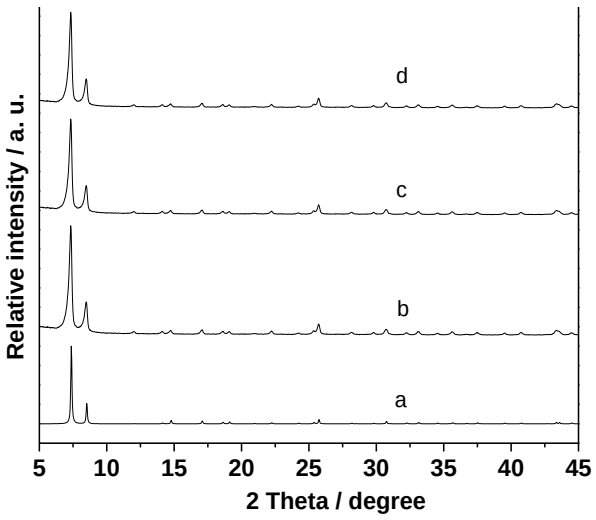

Fig. 1 XRD patterns of UiO-66 simulated from crystal structure data (a), the synthesized NH_2-UiO-66 (b), 2.0 wt.% Pd@NH_2-UiO-66 (c), and the spent 2.0 wt.% Pd@NH_2-UiO-66 catalyst after the sixth-run reaction (d).

Green Chemistry Accepted Manuscript

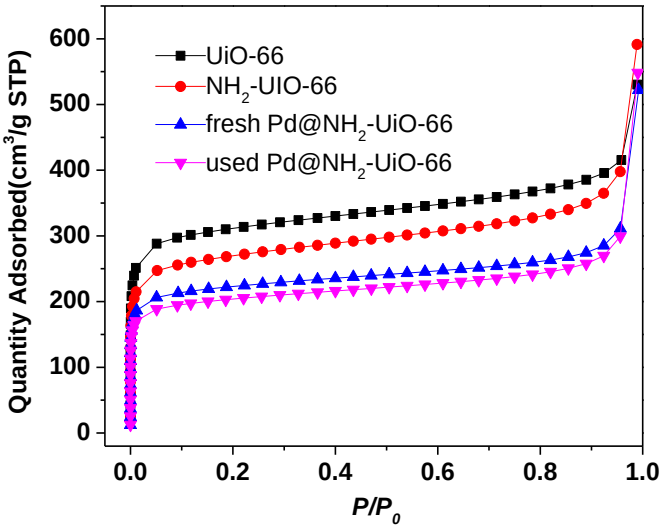

Fig. 2 N_2 adsorption isotherms of unloaded UiO-66 and NH_2-UiO-66 as well as the as prepared (fresh) and the spent (used) Pd@NH_2-UiO-66 catalysts.

The FTIR spectrum shows that the characteristic −OH stretching frequency in the carboxylic acid group of the NH_2-H_2BDC linker centered at 2970 cm^{-1} disappears after formation of the Pd@NH_2-UiO-66 catalyst, suggesting occurrence of the coordination interaction between Zr^{4+} ions and carboxylic acid group of NH_2-H_2BDC to form NH_2-UiO-66 (Fig. 3). In addition, two peaks at around 3470 and 3360 cm^{-1}, attributing to the asymmetric and symmetric stretching absorptions of primary amine group, can be clearly discerned over the prepared NH_2-UiO-66 and Pd@NH_2-UiO-66 (curves b and c in Fig.3). These two peaks are down shifted from 3500 cm^{-1} and 3400 cm^{-1} respectively in comparison with the pure NH_2-H_2BDC (curve a in Fig.3), indicating that the amino groups in the NH_2-UiO-66 are retained [40]. The presence of NH_2 group within the framework of NH_2-UiO-66 was further analyzed using N1s spectra from the XPS data (Fig. S1 in Supporting Information). The N1s peak for amine group appeared at 400 eV.

Green Chemistry Accepted Manuscript

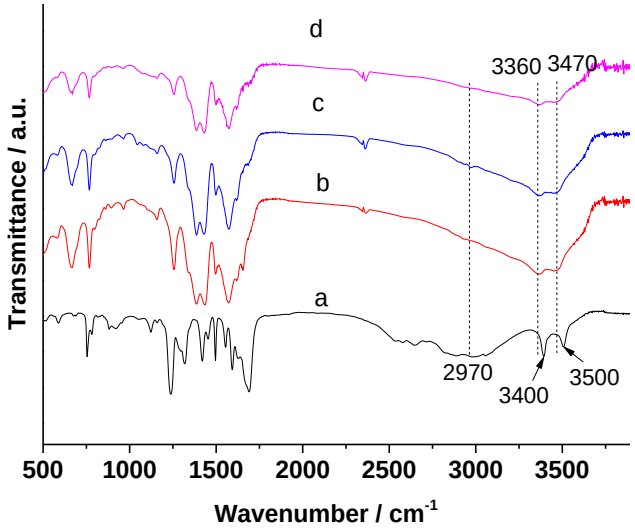

Fig. 3 FTIR spectra of (a) organic linker NH_2-H_2BDC; (b) NH_2-UiO-66; (c) the synthesized Pd@NH_2-UiO-66 and (d) the spent 2.0 wt.% Pd@NH_2-UiO-66 catalyst after the sixth-run reaction.

The loading amount of Pd in (or on) Pd@NH_2-UiO-66 and Pd/NH_2-UiO-66 are 1.97 wt.% and 1.92 wt.%, respectively, as determined by the ICP-AES analysis, very close to the nominal amount of 2.0 wt.%. However, in Pd@UiO-66, only 0.4 wt.% Pd was detected, when we anticipated to introduce 2.0 wt.% Pd on the MOF. The majority of Pd precursor for Pd@UiO-66 was lost during the washing steps (probably due to the weak interaction between UiO-66 and the Pd precursor). These results imply that the amine functional groups in NH_2-UiO-66 can strongly favor the loading of metal nanoparticles as reported in other MOFs [42].

Green Chemistry Accepted Manuscript

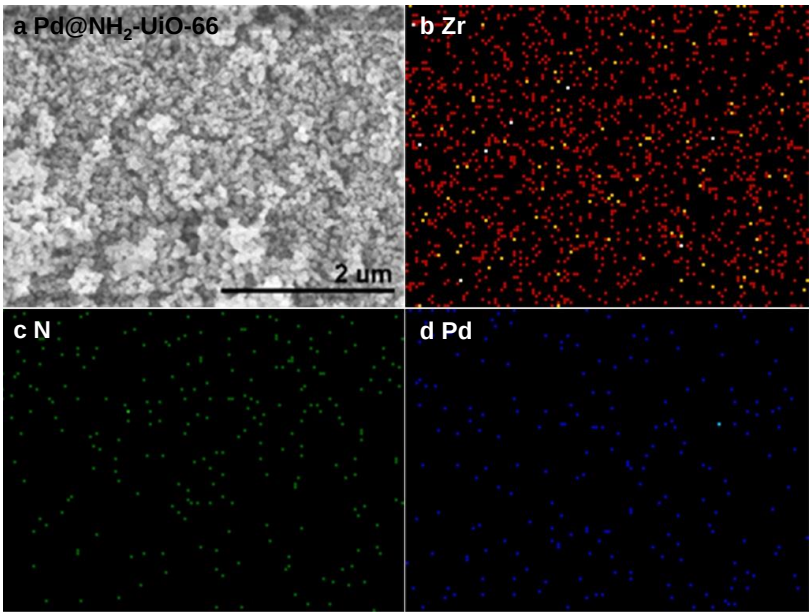

Fig. 4 EDX mapping on the same selected area of the 2.0 wt.% Pd@NH_2-UiO-66.

From the EDX mapping of a selected area on the 2.0 wt.% Pd@NH_2-UiO-66 catalyst, homogeneous distribution of Pd, Zr and N on the same selected area was observed, suggesting that ultrasmall Pd nanoparticles were effectively encapsulated within the NH_2-UiO-66 MOF (Fig. 4). The dispersion was uniform, and no sign of aggregation was observed. The TEM images of the 2.0 wt.% Pd@NH_2-UiO-66 catalyst, shown in Fig. 5, also confirms the uniformity of the Pd nanoparticles in the matrix of NH_2-UiO-66. The sizes of the Pd nanoparticles were mainly within a range of 1.5 – 2.5 nm in diameter, which are well-dispersed (or embedded) inside the cavities of the NH_2-UiO-66 [32]. The slightly larger Pd nanoparticles size than the cage size of NH_2-UiO-66 is probably due to the close contact between Pd nanoparticles with the Zr_6 cluster [24]. It should be noted that the increase of the cage size of NH_2-UiO-66 due to defects in the MOF crystals will facilitate the encapsulation of the Pd nanoparticles within the cages [46,47]. Fig. 5d shows that the Pd nanoparticles are crystalline with a spacing of 0.224 nm, corresponding to the Pd (111) interplanar spacing [31]. On the other hand, the encapsulation of Pd nanoparticles in NH_2-UiO-66 can also be indirectly verified by the hydrogenation of *n*-hexylene and cyclooctene [55], in which 2.0 wt.% Pd@NH_2-UiO-66 had extremely high activity in the hydrogenation of *n*-hexylene for its linear structure making it possible to pass through the narrow window of NH_2-UiO-66. At the same time, the ring reactant (cyclooctene)

Green Chemistry Accepted Manuscript

can barely be converted under the same conditions (Fig. S2). The results indirectly proved that most of the Pd particles are encapsulated by NH_2-UiO-66.

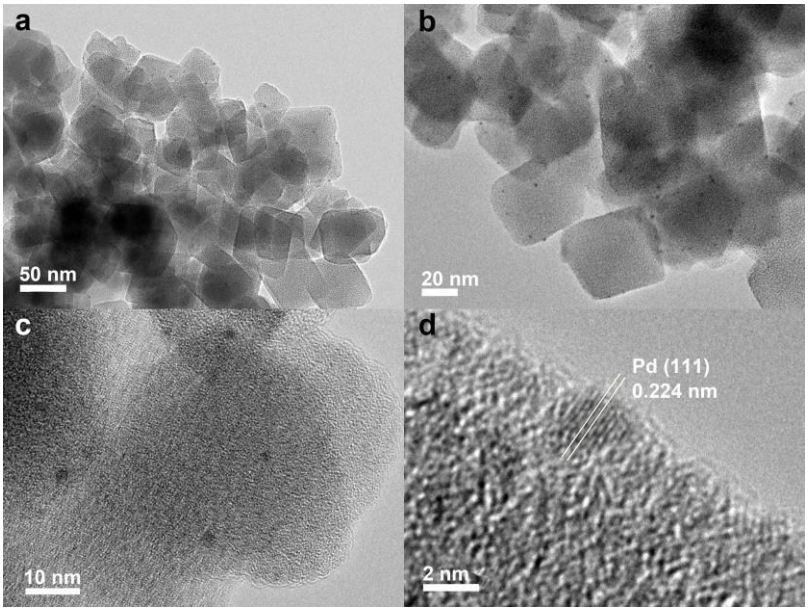

Fig. 5 (a) and (b) TEM images of 2.0 wt.% Pd@NH_2-UiO-66. (c) High resolution image of the 2.0 wt.% Pd@NH_2-UiO-66 catalyst showing that the average size of the Pd nanoparticles is in the range of 1.5 – 2.5 nm. (d) Lattice spacing of the Pd nanoparticle (0.224 nm) corresponding to the Pd (111) interplanar spacing.

The acidities of NH_2-UiO-66 and 2.0 wt.% Pd@NH_2-UiO-66 measured by the NH_3-TPD are shown in Fig. S3. The NH_3-TPD results indicate that the acidity of the NH_2-UiO-66 support can be classified into three groups: weak (110–200 °C), medium (210–300 °C) and strong (330–430 °C), very similar to the results reported by Kim et al [50]. Similarly, the 2.0 wt.% Pd@NH_2-UiO-66 catalyst also exhibits the three kinds of acidic sites, although the desorption temperatures of these acidic sites are slightly offset to low temperatures. On the other hand, it should be noted that the medium acidity sites of the 2.0 wt.% Pd@NH_2-UiO-66 catalyst seem to be much higher than those of the unloaded NH_2-UiO-66 support. Obviously, the major acidity of the 2.0 wt.% Pd@NH_2-UiO-66 catalyst is originated from the accessible metal Zr sites having Lewis acidity [48-51], as well as the

Green Chemistry Accepted Manuscript

defects due to the missing of organic linkers between Zr_6 clusters [46,47]. Furthermore, a portion of the Brønsted acidity can be attributed to the protonation of the amino-functionalized links in the MOF during the synthesis of the 2.0 wt.% Pd@NH_2-UiO-66, with the charge being balanced by chloride anions [42,52]. The IR analysis was conducted for the sample after desorption (Fig. S4). It has been reported that the UiO-66 series of MOFs show exceptionally high thermal stability (up to 450 °C in air) and strong resistance towards water, organic solvents and other chemicals [46,47]. However, compared with parent UiO-66, it should be admitted that thermal stability of NH_2-UiO-66 would decrease to some extent. Nevertheless, the total acid sites number of the 2.0 wt.% Pd@NH_2-UiO-66 catalyst was measured to be 3.0 mmol/g based on the desorbed NH_3.

3.2. Hydrodeoxygenation of vanillin

Considering that water is a desirable green solvent for chemical transformations for reasons of environmental impact, safety and cost, we first conducted the catalytic hydrodeoxygenation in the presence of water. Fig. 6 shows the evolution of the reactant and product contents as a function of reaction time over the 2.0 wt.% Pd@NH_2-UiO-66 catalyst. The reaction was accompanied by a rapid decrease in vanillin and increase in vanillin alcohol in the first 15 min. Later, hydrogenolysis of vanillin alcohol proceeded rapidly.

In general, transformation of a carbonyl group into a methyl group can proceed via three pathways: (1) hydrogenation/dehydration, (2) hydrogenation/hydrogenolysis, and (3) direct hydrogenolysis. Since after hydrogenation vanillin alcohol has no hydrogen atom at the position adjacent to the hydroxyl group, dehydration is not possible in this reaction. Therefore, the transformation of vanillin to 2-methoxy-4-methylphenol must proceed via pathway (2) and/or pathway (3). Fig. 6 illustrates that vanillin is mainly hydrogenated to vanillin alcohol in the first step then converted into 2-methoxy-4-methylphenol.

In order to demonstrate the validity of pathway (2) for the hydrodeoxygenation of vanillin over the 2.0 wt.% Pd@NH_2-UiO-66 catalyst, we further investigated the effect of the reaction temperatures and molar ratios of substrate and catalyst on the conversion and selectivity of vanillin as a function of reaction time. The results are shown in Figs S5 to S8 in Supporting Information. These results consistently prove that the hydrodeoxygenation of vanillin over the 2.0 wt.%

Green Chemistry Accepted Manuscript

Pd@NH_2-UiO-66 catalyst follows pathway (2). Furthermore, it should be noted that 100% conversion of vanillin with exclusive selectivity for 2-methoxy-4-methylphenol could be achieved over the 2.0 wt.% Pd@NH_2-UiO-66 catalyst within 75 min when the reaction was carried out at 90 °C and hydrogen pressure of 0.5 PMa, and no by-product formed even when the reaction time was extended to 300 min (Fig. 6). In contrast, the Pd@UiO-66 catalyst exhibits a low catalytic activity, only 49.3% vanillin was converted and the selectivity for 2-methoxy-4-methylphenol was 43.1% within 70 min (Fig. 7). This can be explained by the limited amount of Pd nanoparticles encaged in the cavities of UiO-66 as determined by ICP-AES.

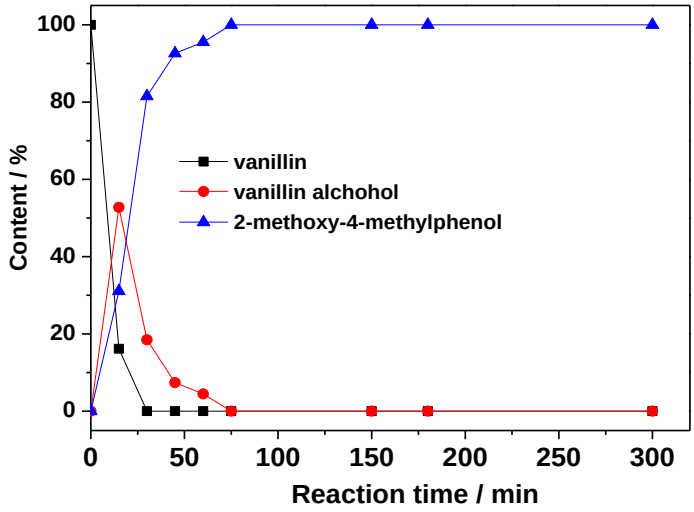

Fig. 6 Changes in the reactant and product distributions as a function of reaction time over 2.0 wt.% Pd@NH_2-UiO-66 catalyst. (Reaction conditions: vanillin, 2 mmol; water, 20 ml; amount of catalyst, 50 mg; S/C = 200; hydrogen pressure, 0.5 MPa; reaction temperature, 90 °C).

On other hand, Pd nanoparticles loaded on the outer surface of NH_2-UiO-66 (2.0 wt.% Pd/NH_2-UiO-66) was also prepared. The TEM images of prepared Pd/NH_2-UiO-66 showed broad distribution of Pd nanoparticles throughout the outer surfaces of NH_2-UiO-66 with an average size of about 5.5 nm (Fig. S9), larger than the cavity size of NH_2-UiO-66. N_2 adsorption measurement of Pd/NH_2-UiO-66 suggested the BET surface and pore volume of the NH_2-UiO-66 framework were almost remained (Table S1). However, the Pd/NH_2-UiO-66 catalyst showed rather low catalytic

Green Chemistry Accepted Manuscript

activity and selectivity, only 74.4% vanillin was converted and the selectivity for 2-methoxy-4-methylphenol was 15.2% when the reaction was carried out at 90 °C for 60 min and hydrogen pressure of 0.5 PMa (Fig. S10), much lower than the counterpart catalyst encapsulated within the cavities of NH_2-UiO-66.

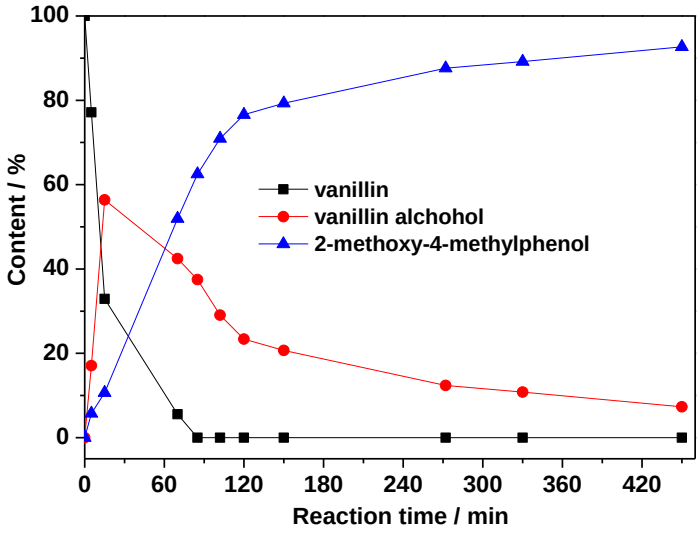

Fig. 7 Changes of reactant and product distributions as a function of reaction time over 0.4 wt.% Pd@UiO-66 (Reaction conditions: vanillin, 2 mmol; water, 20 ml; amount of catalyst, 50 mg; S/C = 1000; hydrogen pressure, 0.5 MPa; reaction temperature, 90 °C).

Additionally, the pH value of the reaction solution using 2.0 wt.% Pd@NH_2-UiO-66 as a catalyst was measured to be in the range of 3.8 to 4.1. As discussed above, The acid sites in UiO-66-NH_2 could be derived from the open Zr(IV) sites, the presence of defects in NH_2-UiO-66 crystals, and a portion of the Brønsted acidity introduced during the catalyst preparation. Whatever the origin of the acid sites is, the presence of acid sites could explain the superior performance of the Pd@NH_2-UiO-66 catalyst for the hydrodeoxygenation of vanillin. Thus, the high catalytic properties of the 2.0 wt.% Pd@NH_2-UiO-66 catalyst in this cascade reaction under mild conditions, is probably correlated to the combination of host-guest cooperation [42,43], where Pd nanoparticles as the guest offer hydrogenation activity and the support host affords acidity as measured by NH_3-TPD, thus promoting the hydrogenolysis. The same promotion effect of Lewis acidity was also observed by Li

Green Chemistry Accepted Manuscript

et al when they conducted the selective hydrogenation of phenol to cyclohexanone in water by using Pd nanoparticles supported onto MIL-101 as catalysts [38].

To provide further evidence for the favorable effect of the acid sites in the NH_2-UiO-66 support for the hydrodeoxygenation, a control experiment was performed over the 2.0 wt.% Pd@NH_2-UiO-66 catalyst in the presence of a stoichiometric amount of NaOH with respect to the number of acid sites available on the catalyst (the amount of acid sites determined by NH_3-TPD) for the hydrogenolysis of vanillin alcohol (the intermediate in the hydrodeoxygenation of vanillin). As can be seen in Fig. S11, the activity of 2.0 wt.% Pd@NH_2-UiO-66 almost fully vanished when the acid sites were poisoned by the presence of NaOH, and this remarkable decrease in catalytic activity is mainly due to the poisoning of the NH_2-UiO-66 active sites by the strong interaction of NaOH with the acid sites of NH_2-UiO-66 [53,54]. This result demonstrates the significant importance of acid sites on the catalytic hydrodeoxygenation.

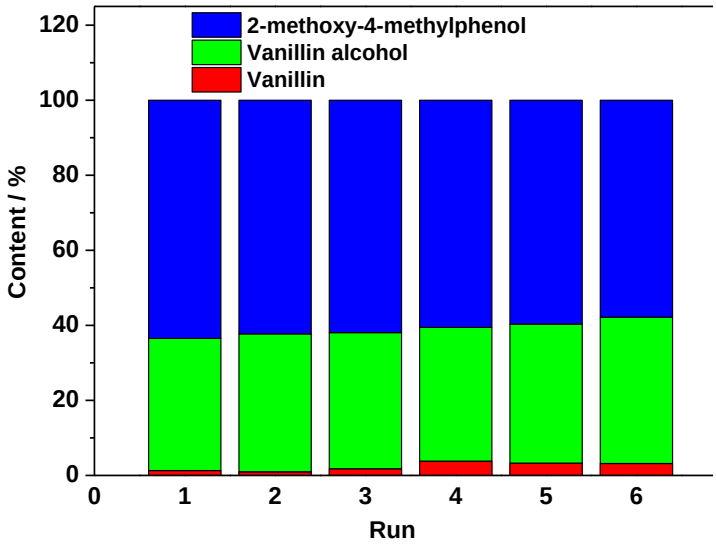

Fig. 8 Reusability of 2.0 wt.% Pd@NH_2-UiO-66 in the catalytic hydrodeoxygenation of vanillin (Reaction conditions: vanillin, 2 mmol; water, 20 ml; amount of catalyst, 50 mg; hydrogen pressure, S/C = 200; 0.5 MPa; reaction temperature, 80 °C; reaction time, 60 min).

More importantly, the 2.0 wt.% Pd@NH_2-UiO-66 catalyst exhibits excellent recyclability (Fig. 8). After being recycled for six times, the catalytic activity and selectivity could be well preserved.

Green Chemistry Accepted Manuscript

The BET surface area of the spent Pd@NH_2-UiO-66 catalyst decreased from 769.2 to 734.7 m^2/g (Fig.2 and Table S1), which may be due to the presence of residual reactants or products trapped inside the NH_2-UiO-66 support. In addition, we measured the XRD pattern of the spent catalysts and found the crystalline structure of the NH_2-UiO-66 was still maintained after the sixth cycle (pattern d in Fig. 1). The corresponding FTIR spectra for the spent catalyst is almost the same as those for the fresh one (curve d in Fig.4). TEM image of used 2.0 wt.% Pd@NH_2-UiO-66 catalyst showed only slight aggregation of Pd nanoparticles (Fig. S12), which does not affect the activity of the catalysts within six repeated cycles. Moreover, the concentration of Pd in the reaction solution was negligible based on the ICP-AES analysis, implying that no Pd leaching occurred during the catalyst repeated reuse.

Moreover, the NH_2-UiO-66 support showed higher adsorption uptake of the substrate and the intermediate than those of UiO-66 (Fig. S13), although the former MOF possesses lower BET specific surface area and pore volume than the latter. It is suggested that the adsorptions of vanillin or vanillin alcohol over amine-functionalized MOFs are enhanced by the hydrophilic nature of substrate molecule as well as the interactions between the substrate molecule and amine-functionalized MOF support [42].

Based on the above discussion, we propose a possible reaction mechanism to illustrate the unique function of the Pd@NH_2-UiO-66 catalyst and demonstrate the reaction sequence for the hydrodeoxygenation of vanillin. In the initial stage, H_2 is presumably activated by the palladium nanoparticles stabilized within the framework of NH_2-UiO-66 [42]. The aldehyde group in vanillin is therefore hydrogenated to the hydroxyl group, and accordingly vanillin is converted into vanillin alcohol. Afterwards, the *in situ* obtained vanillin alcohol is further converted to 2-methoxy-4-methylphenol promoted by acidic sites highly dispersed within the support framework as demonstrated by our controlled experiment.

3.3. Catalytic activity comparison

Furthermore, we compared the catalytic activity and selectivity over the developed 2.0 wt.% Pd@NH_2-UiO-66 catalyst with those reported in the literatures (Table 2). As can been see, a 100% conversion of vanillin with 100% selectivity for 2-methoxy-4-methylphenol could be obtained over

Green Chemistry Accepted Manuscript

2.0 wt.% Pd@NH_2-UiO-66 within 60 min (entry 1 in Table 2). The selectivity for 2-methoxy-4-methylphenol over the prepared 2.0 wt.% Pd@NH_2-UiO-66 is much higher than the result reported by Xiao et al over 4.5 wt.% Pd/MSMF under the same reaction conditions with a similar conversion of vanillin [15] (entry 2), as well as higher than 2.0 wt.% Pd/SO_3H-MIL-101 [56] (entry 3). Additionally, 2.0 wt.% Pd@NH_2-UiO-66 is also superior to the N-doped carbon-supported Pd catalyst [14] (entries 4 and 5) and 2.0 wt.% Pd@MIL-101 [57] (entries 6 and 7). On the other hand, Resasco and co-workers found that an 85% conversion of vanillin within 0.5 h with 47% selectivity (entry 8) for 2-methoxy-4-methylphenol could be achieved in the hydrodeoxygenation of vanillin by depositing palladium onto SWNT-inorganic oxide hybrid (Pd/SWNT-SiO_2) in a water/oil system [13]. In contrast, our 2.0 wt.% Pd@NH_2-UiO-66 showed remarkably high catalytic activity and selectivity for 2-methoxy-4-methylphenol under the same conditions (entry 9). The superior performance for Pd@NH_2-UiO-66 is mainly due to the cooperation between the well-dispersed metallic Pd sites and the amine-functionalized MOFs promoted by the acidity highly distributed throughout the framework of NH_2-UiO-66.

Table 2. Hydrodexygenation of vanillin over different catalysts

Entry	Catalyst	Conversion (%)	Selectivity (%)[a]	
			B	C
1[b]	2.0 wt.% Pd@NH_2-UiO-66	100	0	100
2[b]	4.5 wt.% Pd/MSMF [15]	> 99.5	45.8	54.2
3[b]	2.0 wt.% Pd/SO_3H-MIL-101 [56]	96.1	9.1	90.9
4[c]	2.0 wt.% Pd@NH_2-UiO-66	99.1	21.4	78.6
5[c]	Pd/$CN_{0.132}$ [14]	65	31	69
6[d]	2.0 wt.% Pd@NH_2-UiO-66	100	0	100
7[d]	2.0 wt.% Pd@MIL-101 [57]	50	2	98
8[e]	5.0 wt.% Pd/SWNT-SiO_2 [13]	85	53	47
9[e]	2.0 wt.% Pd@NH_2-UiO-66	100	24.8	75.2

[a]B is the hydrogenation product, vanillin alcohol, and C is the hydrogenolysis product, 2-methoxy-4-methylphenol (see Scheme 1).

[b]Reaction conditions: water, 20 ml; S/C (molar ratio of substrate to catalyst) = 200; 0.5 MPa; reaction temperature, 100 °C; reaction time, 60 min.

[c]Reaction conditions: water, 80 ml; S/C = 350; hydrogen pressure, 1.0 MPa; reaction temperature, 90 °C; reaction time, 60 min.

[d]Reaction conditions: water, 5 ml; S/C = 35; hydrogen pressure, 0.2 MPa; reaction temperature,

Green Chemistry Accepted Manuscript

75 °C; reaction time, 60 min.

[e]Reaction conditions: 1:1 (v/v) water/decalin, 20 ml; S/C = 100; hydrogen pressure, 0.35 MPa; reaction temperature, 100 °C; reaction time, 30 min.

4. Conclusions

In summary, we have developed an efficient heterogeneous catalyst consist of ultrasmall palladium nanoparticles immobilized on amine-functionalized metal−organic frameworks (2.0 wt.% Pd@NH_2-UiO-66) by using a direct anionic exchange and subsequent gentle reduction approach. The presence of free amine moieties in the frameworks of Pd@NH_2-UiO-66 is assumed to play a key role on the formation of uniform, well dispersed and leaching resistant palladium nanoparticles on the support. The prepared Pd@NH_2-UiO-66 catalyst exhibits excellent catalytic properties in the hydrodeoxygenation of vanillin in aqueous media. The superior performance for Pd@NH_2-UiO-66 is due to the cooperation between the metallic Pd sites and the amine-functionalized MOFs. The research thus highlights new perspectives for amine-functionalized MOF material for biomass transformation.

Acknowledgements

This work was supported by National Natural Science Foundation of China (21576243, 21471131), and Zhejiang Provincial Natural Science Foundation of China (LY13B030002).

References

1. D. Sutton, F. D. Waldie, R. Wu, M. Schlaf, L. A. ‘Pete’ Silks and J. C. Gordon, *Nat. Chem.*, 2013, 5, 428–432.
2. L. Petrus and M. A. Noordermeer, *Green Chem*., 2006, 8, 861–867.
3. C. Zhao, Y. Kou, A. A. Lemonidou, X. B. Li and J. A. Lercher, *Angew. Chem. Int. Ed*., 2009, 48, 3987–3990.
4. J. Y. He, C. Zhao and J. A. Lercher, *J. Am. Chem. Soc*., 2012, 134, 20768–20775.
5. S. De, B. Saha and R. Luque, *Bioresour. Technol.*, 2015, 178, 108–118.
6. M. Saidi, F. Samimi, D. Karimipourfard, T. Nimmanwudipong, B. C. Gates and M. R. Rahimpour, *Energy Environ. Sci.*, 2014, 7, 103–129.

Green Chemistry Accepted Manuscript

7. H. Zacher, M. V. Olarte, D. M. Santosa, D. C. Elliott and S. B. Jones, *Green Chem.*, 2014, 16, 491–515.
8. J. Yang, C. L. Williams, A. Ramasubramaniam and P. J. Dauenhauer, *Green Chem.*, 2014, 16, 675–682.
9. P. T. M. Do, A. J. Foster, J. Chen and R. F. Lobo, *Green Chem.*, 2012, 14, 1388–1397.
10. X. Xu, Y. Li, Y. Gong, P. Zhang, H. Li and Y. Wang, *J. Am. Chem. Soc.*, 2012, 134, 16987–16990.
11. X. Yang, Y. Liang, Y. Cheng, W. Song, X. Wang, Z. Wang and J. Qiu, *Catal. Commun.*, 2014, 47, 28–31.
12. X. Yang, Y. Liang, X. Zhao, Y. Song, L. Hu, X. Wang, Z. Wang and J. Qiu, *RSC Adv.*, 2014, 4, 31932–31936.
13. Z. Zhu, H. Tan, J. Wang, S. Yu and K. Zhou, *Green Chem.*, 2014, 16, 2636–2643.
14. S. Crossley, J. Faria, M. Shen and D. E. Resasco, *Science*, 2010, 327, 68–72.
15. Z. Lv, Q. Sun, X. Meng and F. S. Xiao, *J. Mater. Chem. A*, 2013, 1, 8630–8635.
16. S. Jin, Z. Xiao, C. Li, X. Chen, L. Wang, J. Xing, W. Li and C. Liang, *Catal. Today*, 2014, 234, 125–132.
17. S. Jin, Z. Xiao, X. Chen, L. Wang, J. Guo, M. Zhang and C. Liang, *Ind. Eng. Chem, Res.*, 2015, 54, 2302–2310.
18. M. Yaghi, M. O'Keeffe, N. W. Ockwig, H. K. Chae, M. Eddaoudi and J. Kim, *Nature*, 2003, 423, 705–714.
19. N. Stock and S. Biswas, *Chem. Rev.*, 2012, 112, 933–969.
20. A. Corma, H. García and F. X. Llabrés i Xamena, *Chem. Rev.*, 2010, 110, 4606–4655.
21. S. Kitagawa, R. Kitaura and S. Noro, *Angew. Chem. Int. Ed.*, 2004, 43, 2334–2375.
22. C. Rosler and R. A. Fischer, *CrystEngComm*, 2015, 17, 199–217.
23. A. Aijaz, A. Karkamkar, Y. J. Choi, N. Tsumori, E. Rönnebro, T. Autrey, H. Shioyama and Q. Xu, *J. Am. Chem. Soc.*, 2012, 134, 13926–13929.
24. H. Khajavi, H. A. Stil, H. P. C. E. Kuipers, J. Gascon and F. Kapteijn, *ACS Catal.*, 2013, 3, 2617–2626.
25. M. Meilikhov, K. Yusenko, D. Esken, S. Turner, G. Van Tendeloo and R. A. Fischer, *Eur. J.*

Green Chemistry Accepted Manuscript

Inorg. Chem., 2010, 2010, 3701–3714.

26. L. Chen, H. Chen, R. Luque and Y. Li, *Chem. Sci.*, 2014, 5, 3708–3714.
27. Z. Guo, C. Xiao, R. V. Maligal-Ganesh, L. Zhou, T. W. Goh, X. Li, D. Tesfagaber, A. Thiel and W. Huang, *ACS Catal.*, 2014, 4, 1340–1348.
28. K. Na, K. M. Choi, O. M. Yaghi and G. A. Somorjai, *Nano Lett.*, 2014, 14, 5979–5983.
29. M. S. El-Shall, V. Abdelsayed, A. Khder, H. M. A. Hassan, H. M. El-Kaderi and T. E. Reich, *J. Mater. Chem.*, 2009, 19, 7625–7631.
30. A. Aijaz and Q. Xu, *J. Phys. Chem. Lett.*, 2014, 5, 1400–1411.
31. X. Zhao, Y. Jin, F. Zhang, Y. Zhong and W. Zhu, *Chem. Eng. J.*, 2014, 239, 33–41.
32. H. Li, Z. Zhu, F. Zhang, S. Xie, H. Li, P. Li and X. Zhou, *ACS Catal.*, 2011, 1, 1604–1612
33. J. Long, H. Liu, S. Wu, S. Liao and Y. Li, *ACS Catal.*, 2013, 3, 647–654.
34. V. Pascanu, Q. Yao, A. Bermejo Gómez, M. Gustafsson, Y. Yun, W. Wan, L. Samain, X. Zou and B. Martín-Matute, *Chem. Eur. J.*, 2013, 19, 17483–17493.
35. A. Dhakshinamoorthy and H. Garcia, *Chem. Soc. Rev.*, 2012, 41, 5262–5284.
36. J. Juan-Alcañiz, J. Ferrando-Soria, I. Luz, P. Serra-Crespo, E. Skupien, V. P. Santos, E. Pardo, F. X. Llabrés i Xamena, F. Kapteijn and J. Gascon, *J. Catal.*, 2013, 307, 295–304.
37. Y. Pan, B. Yuan, Y. Li and D. He, *Chem. Commun.*, 2010, 46, 2280–2282.
38. H. Liu, Y. Li, R. Luque and H. Jiang, *Adv. Synth. Catal.*, 2011, 353, 3107–3113.
39. F. G. Cirujano, F. X. Llabres i Xamena and A. Corma, *Dalton Trans.*, 2012, 41, 4249–4254.
40. M. Zhao, K. Deng, L. He, Y. Liu, G. Li, H. Zhao and Z. Tang, *J. Am. Chem. Soc.*, 2014, 136, 1738–1741.
41. Y. Z. Chen, Y. X. Zhou, H. Wang, J. Lu, T. Uchida, Q. Xu, S. H. Yu and H. L. Jiang, *ACS Catal.*, 2015, 5, 2062–2069.
42. J. Chen, R. Liu, Y. Guo, L. Chen and H. Gao, *ACS Catal.*, 2015, 5, 722–733.
43. X. Li, Z. Guo, C. Xiao, T. W. Goh, D. Tesfagaber and W. Huang, *ACS Catal.*, 2014, 4, 3490–3497.
44. A. Dhakshinamoorthy and H. Garcia, *ChemSusChem*, 2014, 7, 2392–2410.
45. J. Gascon, A. Corma, F. Kapteijn and F. X. Llabrés i Xamena, *ACS Catal.*, 2014, 4, 361–378.
46. J. H. Cavka, S. Jakobsen, U. Olsbye, N. Guillou, C. Lamberti, S. Bordiga and K. P. Lillerud, *J.*

Green Chemistry Accepted Manuscript

Am. Chem. Soc., 2008, 130, 13850–13851.

47. A. Schaate, P. Roy, A. Godt, J. Lippke, F. Waltz, M. Wiebcke and P. Behrens, *Chem. Eur. J.*, 2011, 17, 6643–6651.
48. Y. Yang, H. F. Yao, F. G. Xi and E. Q. Gao, *J. Mol. Catal. A*, 2014, 390, 198–205.
49. V. N. Panchenko, M. M. Matrosova, J. Jeon, J. W. Jun, M. N. Timofeeva and S. H. Jhung, *J. Catal.*, 2014, 316, 251–259.
50. J. Kim, S. N. Kim, H. G. Jang, G. Seo and W. S. Ahn, *Appl. Catal. A.*, 2013, 453, 175–180.
51. F. G. Cirujano, A. Corma and F. X. Llabrés i Xamena, *Catal. Today*, 2015, 257, 213–220.
52. W. Morris, C. J. Doonan and O. M. Yaghi, *Inorg. Chem.*, 2011, 50, 6853–6855.
53. Y.Z. Chen, Y.X. Zhou, H. Wang, J. Lu, T. Uchida, Q. Xu, S.H. Yu and H.L. Jiang, *ACS Catal.*, 2015, 5, 2062–2069.
54. F. Zhang, J. Shi, Y. Jin, Y. Fu, Y. Zhong and W. Zhu, *Chem. Eng. J.*, 2015, 259, 183–190.
55. M. Zhang, Y. Yang, C. Li, Q. Liu, C. T. Williams and C. Liang, *Catal. Sci. Technol.*, 2014, 4, 329–332.
56. F. Zhang, Y. Jin, Y. Fu, Y. Zhong, W. Zhu, A. Ibrahim and M. S. El-Shall, *J. Mater. Chem. A*, 2015, 3, 17008–17015.
57. A. Aijaz, Q. L. Zhu, N. Tsumori, T. Akita and Q. Xu, *Chem. Commun.*, 2015, 51, 2577–2580.

Green Chemistry Accepted Manuscript

Graphical Abstract

Synergetic Catalysis of Palladium Nanoparticles Encaged within Amine-functionalized UiO-66 in Hydrodeoxygenation of Vanillin in Water

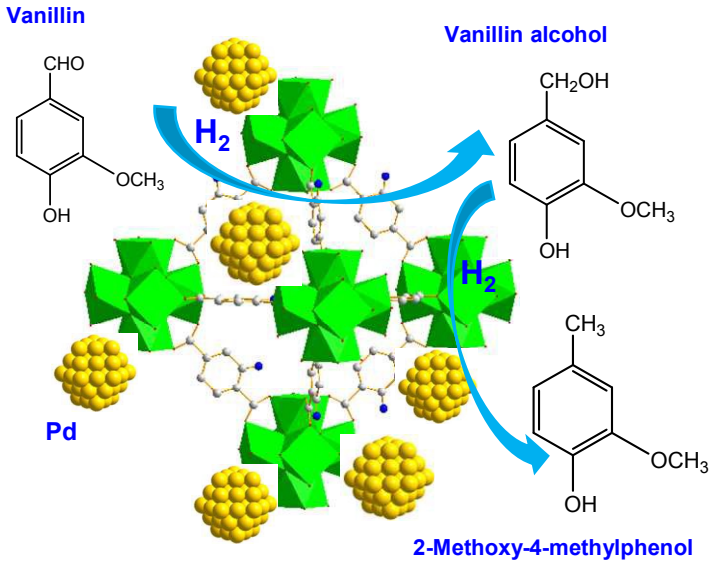

Green Chemistry Accepted Manuscript